

TRACING THE SHOCK PRECURSORS IN THE L1448-MM/IRS3 OUTFLOWS

I. JIMÉNEZ-SERRA, J. MARTÍN-PINTADO AND A. RODRÍGUEZ-FRANCO¹

Instituto de Estructura de la Materia (CSIC),
Departamento de Astrofísica Molecular e Infrarroja,
C/ Serrano 121, E-28006 Madrid, Spain

AND

N. MARCELINO

Instituto de RadioAstronomía Milimétrica
Avda. Divina Pastora 7, Núcleo Central, E-18012 Granada, Spain

Draft version November 24, 2018

ABSTRACT

We present the detection of the SiO $\nu=0$ $J=2-1$ and $J=3-2$ lines, and of the HCO $1_{01}-0_{00}$ $J=3/2-1/2$ $F=2-1$ line at ambient velocities towards the molecular outflows in L1448-mm and L1448-IRS3. This is the first detection of HCO in a dark cloud. We have also measured lines of H^{13}CO^+ , H^{13}CN , HN^{13}C , CH_3OH , and N_2H^+ . While the HCO and the SiO lines have the narrowest profiles with linewidths of $\sim 0.5 \text{ km s}^{-1}$, the other lines have widths of $\sim 1 \text{ km s}^{-1}$. Towards L1448-mm, all lines except those of SiO and HCO, show two distinct velocity components centered at 4.7 and 5.2 km s^{-1} . HCO is only observed in the 4.7 km s^{-1} cloud, and SiO in the 5.2 km s^{-1} component. The SiO abundance is $\sim 10^{-11}$ in the 5.2 km s^{-1} clouds, one order of magnitude larger than in the 4.7 km s^{-1} component and in other dark clouds. The HCO abundance is $\sim 10^{-11}$, similar to that predicted by the ion-molecule reactions models for the quiescent gas in dark clouds. The large change in the SiO/HCO abundance ratio (>150) from the 4.7 to the 5.2 km s^{-1} component, and the distribution and kinematics of the SiO emission towards L1448-mm suggest that the ambient SiO is associated with the molecular outflows. We propose that the narrow linewidths and the abundances of SiO in the ambient gas are produced by the interaction of the magnetic and/or radiative precursors of the shocks with the clumpy pre-shocked ambient gas.

Subject headings: stars: formation — ISM: individual (L1448) — ISM: jets and outflows — ISM: molecules — ISM: structure

1. INTRODUCTION

It is well-known that the SiO emission traces the material which has been processed by shocks. The SiO profiles present very broad linewidths that are centered at velocities different from that of the ambient cloud (Martín-Pintado, Bachiller, & Fuente 1992). As silicon is heavily depleted onto dust grains in the cold quiescent gas, the SiO abundances are extremely low in dark clouds ($\leq 10^{-12}$; Ziurys, Friberg, & Irvine 1989; Martín-Pintado et al. 1992). Nevertheless, Lefloch et al. (1998) reported the first detection of bright and narrow (with the same linewidth of the ambient gas) SiO lines at ambient velocities associated with the molecular outflows in the dark cloud NGC 1333 ($t > 10^4$ years). Lefloch et al. (1998) suggested that the SiO emission arises from the postshock equilibrium gas after the interaction of powerful protostellar jets with local dense clumps. They concluded that the narrow SiO emission could be only detected in particular objects characterized by its high degree of clumpiness. Codella, Bachiller, & Reipurth (1999) confirmed the suggestion of Lefloch et al. (1998) that the ambient SiO emission arises from decelerated postshock material. In this scenario one would not expect to detect SiO ambient emission with narrow linewidths in very young molecular outflows.

The L1448 outflow is a very young outflow with a dynamical age of only ~ 3500 years (Bachiller et al. 1990). Due its youth, this object provides an excellent laboratory to study the origin of the ambient SiO emission, because the time scale is too short for the postshock gas to reach the equilibrium (Chièze, Pineau des Forêts, & Flower 1998) and to decelerate to the radial velocities of those of the ambient gas.

The formyl radical (HCO) has not been detected so far in dark clouds (e.g. L183, where the derived HCO abundance is $< 2 \times 10^{-10}$; Schenewerk et al. 1988). However, gas-phase chemistry models predict even lower HCO abundances ($\sim 10^{-11}$) than the previously measured upper limits to this molecule (Leung, Herbst, & Huebner 1984).

In this Letter we present the first detection of very narrow SiO and HCO emissions at ambient velocities in the L1448-mm/IRS3 molecular outflows. The narrow lines and the radial velocities of the SiO emission do not seem to be related to decelerated postshock equilibrium gas but produced by the interaction of the magnetic and/or radiative shock-precursors with the ambient pre-shocked clumpy medium.

2. OBSERVATIONS AND RESULTS

The observations were carried out with the IRAM 30-m telescope at Pico Veleta (Spain). We observed the central position of L1448-mm (the driving source of the highly collimated outflow) and L1448-IRS3, and

¹ Escuela Universitaria de Óptica, Departamento de Matemática Aplicada (Biomatemática), Universidad Complutense de Madrid, Avda. Arcos de Jalón s/n, E-28037 Madrid, Spain

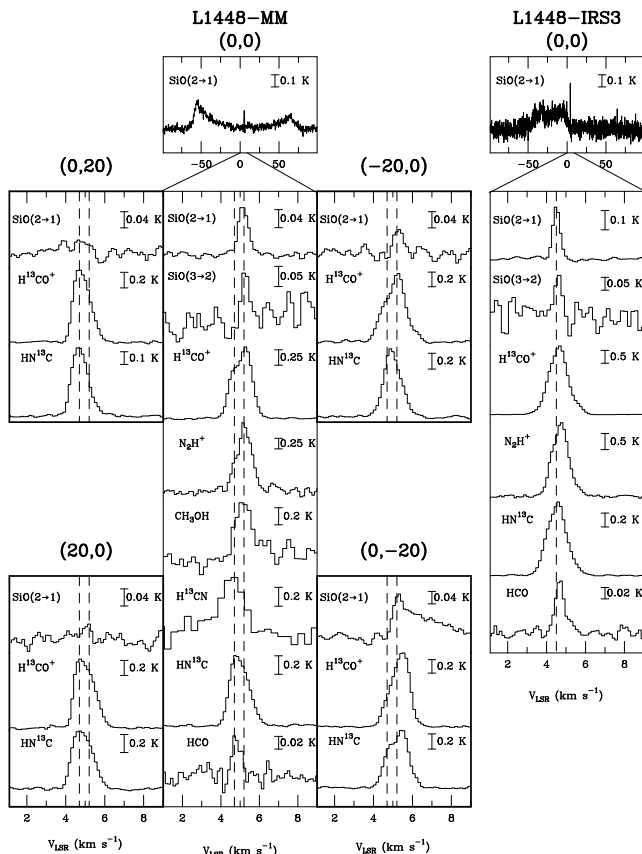


FIG. 1.— Sample of line profiles for the different positions towards the L1448-mm/IRS3 molecular outflows. The offsets, in arcseconds at the top of the panels, refer to the position of L1448-mm ($\alpha(2000) = 03^{\text{h}}25^{\text{m}}38^{\text{s}}.0$, $\delta(2000) = 30^{\circ}44'05''$). The dashed vertical lines show the radial velocities of the velocity components for which SiO and HCO have been detected.

mapped the L1448-mm region observing towards the offsets (20,0), (-20,0), (0,20), and (0,-20). Table 1 summarizes the parameters of the observed transitions. The beam size of the telescope was $\sim 27''$ at ~ 90 GHz and $\sim 18''$ at ~ 140 GHz. The 3 mm and the 2 mm SIS receivers were tuned to single side band with image rejections >10 dB. We observed simultaneously the SiO $J=2-1$, H^{13}CO^+ , HN^{13}C , and HCO species using the frequency-switching mode with a frequency throw of 3 MHz. As spectrometers we used VESPA, which provided a velocity resolution of ~ 0.14 km s^{-1} . Typical system temperatures were 90–100 K. We observed the rest of the species (H^{13}CN , CH_3OH , N_2H^+ , and the SiO $J=3-2$ transition) in position-switching mode. The system temperatures and the spectral resolutions were typically of 120–350 K and 0.13–0.20 km s^{-1} , respectively. All the line intensities were calibrated in antenna temperature.

Fig. 1 shows all the spectra measured for the L1448-mm map and L1448-IRS3, and Table 1 shows the observed parameters for all the lines measured towards the central positions in L1448-mm and L1448-IRS3. For comparison, Fig. 1 shows, in the upper panels, the profiles of the blueshifted and redshifted shocked gas with broad, ~ 50 km s^{-1} , lines (see e.g., Martín-Pintado et al. 1992). The ambient profiles are shown in detail in the central panels of Fig. 1. The SiO and HCO ambient emissions show very narrow linewidths of

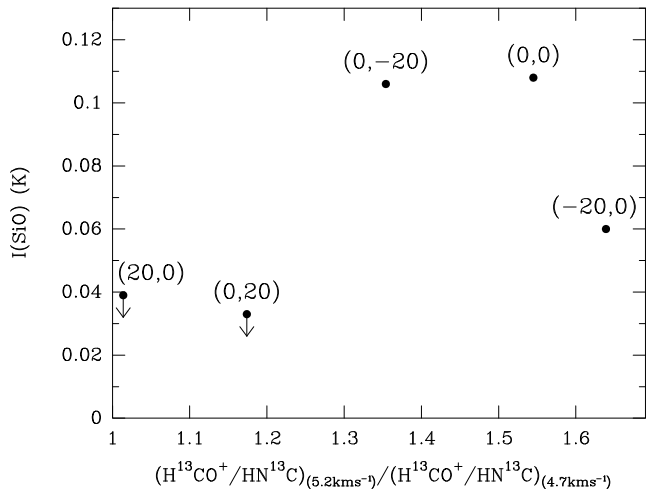


FIG. 2.— Correlation between the narrow SiO emission intensity and the ion (H^{13}CO^+) to neutral (HN^{13}C) intensity ratio for the 5.2 and 4.7 km s^{-1} velocity components detected towards the positions mapped in L1448-mm (the position offsets shown above the points are relative to L1448-mm). The vertical arrows indicate upper limits to the SiO emission. Note the trend of the relative ion to neutral abundance to increase at the positions where SiO has been detected.

~ 0.5 km s^{-1} , smaller than those of the ambient cloud molecules like H^{13}CO^+ , HN^{13}C , and N_2H^+ which have widths of ~ 1 km s^{-1} . There are appreciable differences between the observed profiles of SiO, HCO, and the other molecules. While all ambient molecules towards L1448-mm show double peaked profiles with velocity peaks at 4.7 and 5.2 km s^{-1} (see vertical dashed lines in Fig. 1), the HCO and SiO lines are single gaussian narrow profiles with peaks at 4.7 and 5.2 km s^{-1} respectively (Table 1). VLA images of the ambient NH_3 gas show that these two components correspond to distinct molecular clumps with different spatial distribution associated with the L1448-mm source (Curiel et al. 1999).

From our limited map, we notice that the detection of the SiO emission in the 5.2 km s^{-1} cloud is related to an increase of the ion abundance with respect to neutrals. Fig. 2 illustrates this effect by representing the SiO line intensities as a function of the ratio between the ion (H^{13}CO^+) and the neutral (HN^{13}C) intensities for the 4.7 and the 5.2 km s^{-1} components. Although the data are scarce, the tendency of the SiO emission to increase with the ion to neutral intensity ratio is clear. Since the lines are optically thin, this shows that the larger SiO abundance in the ambient cloud is associated with an enhancement of the ion abundance relative to the neutrals. Furthermore, we find that the SiO profile towards L1448-mm (0,-20) presents a substantial broadening (redshifted with respect to the ambient gas) due to material which has already entered the shock. Although CH_3OH is also a neutral molecule, its emission is shifted to the 5.2 km s^{-1} component. As discussed in section 4, these data are consistent with the fact that the SiO and CH_3OH abundances are enhanced by grain mantle destruction produced by shocks (Millar, Herbst, & Charnley 1991).

Towards L1448-IRS3, we have measured the strongest narrow SiO emission in L1448. Again, the SiO and HCO lines are narrower (with linewidths ~ 0.5 km s^{-1}) than

TABLE 1

Line	L1448–mm			L1448–IRS3		
	Intensity ^d (K)	V_{LSR} (km s ⁻¹)	Δv (km s ⁻¹)	Intensity (K)	V_{LSR} (km s ⁻¹)	Δv (km s ⁻¹)
SiO(2 → 1)	0.108 (5) ≤0.015	5.168 (9) ~4.7	0.62 (2)	0.275 (5)	4.503 (4)	0.437 (9)
SiO(3 → 2)	0.14 (4) ≤0.096	5.29 (6) ~4.7	0.6 (2)	0.173 (7)	4.38 (5)	0.5 (1)
H ¹³ CO ⁺ (1 → 0)	1.150 (8) 0.636 (8)	5.298 (7) 4.585 (8)	0.81 (1) 0.59 (2)	2.58 (7)	4.610 (1)	1.159 (1)
N ₂ H ⁺ (1 → 0) ^a	1.49 (6) 0.29 (6)	5.25 (1) 4.61 (3)	0.84 (3) 0.28 (7)	2.22 (8)	4.7 (1)	1.0 (3)
HCO(1 ₀₁ → 0 ₀₀) ^b	≤0.03 0.059 (8)	~5.2 4.81 (4)	0.49 (7)	0.094 (4)	4.68 (5)	0.5 (1)
HN ¹³ C (1 → 0) ^c	0.559 (5) 0.428 (5)	5.16 (4) 4.64 (1)	1.03 (3) 0.62 (3)	1.02 (3)	4.532 (2)	1.187 (4)
H ¹³ CN (1 → 0) ^c	≤0.30 0.40 (5)	~5.2 4.56 (9)	1.5 (2)			
CH ₃ OH(3 ₀ → 2 ₀ A ⁺)	0.65 (6) ≤0.40	5.20 (5) ~4.7	1.1 (1)			

^aRefers to the $F = 0 \rightarrow 1$ hyperfine component.

^bRefers to the $J = 3/2 \rightarrow 1/2$, $F = 2 \rightarrow 1$ transition.

^cRefers to the $F = 2 \rightarrow 1$ hyperfine component.

^dIntensities are in antenna temperature. The limits correspond to 3σ .

those of the ambient molecules. Toward this position all line profiles are single peaked, but the SiO emission shows an appreciable velocity shift relative to the emissions from ambient molecules (~ 0.2 km s⁻¹; see vertical line in Fig. 1). Like in L1448–mm, this narrow emission is shifted in the same velocity direction as the shocked material which suggests that the "ambient" SiO is related to shocks.

3. ABUNDANCES

Assuming a kinetic temperature of 20 K (Curiel et al. 1999), Table 2 shows the derived H₂ densities and the column densities of all molecules for the central region of L1448–mm and L1448–IRS3. The H₂ densities derived from the SiO $J=2-1$ and $J=3-2$ lines are a few 10^5 – 10^6 cm⁻³. If we consider a HCO⁺ fractional abundance of $\sim 10^{-8}$ (Irvine et al. 1987), the derived SiO abundance towards L1448–mm (0,0), (-20,0), and (0,-20) is $\sim 10^{-11}$ for the 5.2 km s⁻¹ component, an order of magnitude lower than what Lefloch et al. (1998) found in NGC 1333. The estimated upper limit to the SiO abundance for the 4.7 km s⁻¹ cloud is $\leq 10^{-12}$ at L1448–mm (0,0), of the same order as that obtained in the cold quiescent clouds TMC1 and B1 (Ziurys et al. 1989; Martín-Pintado et al. 1992). Therefore, the SiO abundance in the 5.2 km s⁻¹ component has been enhanced by more than one order of magnitude with respect to the quiescent gas of the 4.7 km s⁻¹ cloud.

On the other hand, HCO has not been detected for the 5.2 km s⁻¹ component (Fig. 1), with an upper limit of $\chi(\text{HCO}) \leq 4 \times 10^{-12}$ (Table 2). For the 4.7 km s⁻¹ cloud, we derive a HCO abundance of few 10^{-11} .

4. DISCUSSION

HCO is predicted to be produced in dark clouds through ion–molecule reactions with abundances of 10^{-11} (Leung et al. 1984). Our detection of HCO and the abundances derived for this molecule ($\sim 10^{-11}$, Table 2) are in agreement with these models, suggesting that the 4.7 km s⁻¹ material traces the quiescent gas.

The SiO/HCO abundance ratio changes by more than two orders of magnitude from the 4.7 to the 5.2 km s⁻¹ component of the ambient gas, indicating that the formation of both molecules are related to different mechanisms.

The spatial distribution and the kinematics of the narrow SiO emission suggest that this emission is associated with the molecular outflows towards L1448–mm and L1448–IRS3. However, the lines are very narrow and with the radial velocities of the ambient gas. We can rule out the idea that the ambient SiO emission is generated in the postshock equilibrium gas since the time scales for the shocked gas to decelerate to the ambient velocities are much larger ($\geq 10^4$ years) than the dynamical age, and the SiO has not been detected in the ambient 4.7 km s⁻¹ cloud.

In the following, we explore the possibility that the SiO ambient emission is a signature of the shock precursors associated with the jets driven by the young stars. There is a tendency for the ambient SiO emission to arise only from regions where the relative abundance of the ions to neutrals is larger than in the quiescent clumps (see Fig. 1). This indicates that the ions could have slipped to the 5.2 km s⁻¹ component from the neutrals of the 4.7 km s⁻¹ cloud, as expected if this narrow emission were produced by the magnetic precursor associated with C–type shocks. The magnetic precursor would force the plasma to stream through the neutral gas ahead the jump front, generating a velocity decoupling between the charged and neutral fluids (Draine 1980). As the charged particles were compressed in the first stages of the magnetic precursor, the ion density would initially increase in the 5.2 km s⁻¹ component with respect to the quiescent 4.7 km s⁻¹ cloud (see e.g. Flower et al. 1996).

Pilipp, Hartquist, & Havnes (1990) and Pilipp & Hartquist (1994) have considered grains as a separated fluid from the ion, neutral, and electron components. The behavior of the grains changes depending on several parameters like the H₂ density, mean charge, and grain

TABLE 2

Source	H ₂ density 10 ⁵ (cm ⁻³)	Column density (10 ¹² cm ⁻²)						χ(SiO)	χ(HCO)
		SiO	HCO	H ¹³ CO ⁺	HN ¹³ C	CH ₃ OH	N ₂ H ⁺		
L1448-mm (5.2 km s ⁻¹)	~10	0.2	≤0.03	1.0	1.0	80	20	1×10 ⁻¹¹	≤4×10 ⁻¹²
L1448-mm (4.7 km s ⁻¹)	~10	≤0.004	0.2	0.4	0.5	≤30	1.1	≤1×10 ⁻¹²	6×10 ⁻¹¹
L1448-IRS3	2.4	0.3	0.4	2.8	1.7		40	1×10 ⁻¹¹	2×10 ⁻¹¹

NOTE. — Abundance upper limits were estimated from the 3σ level. These parameters have been derived for the central region in each source.

size distribution. There are cases where the charged grains are coupled to the ions, leading to a small grain-neutral velocity drift just before the shock starts. The Chièze et al. (1998) time-dependent C-shock model shows that, even for time scales of <10⁴ years, this velocity drift generates the sufficient friction to produce the ejection of small amounts of silicon from grains into the gas phase in the 5.2 km s⁻¹ cloud through sputtering (Flower et al. 1996; Caselli, Hartquist, & Havnes 1997). Since these time scales are rather short, we should expect that silicon is released directly in the form of SiO, producing an abundance of 10⁻¹⁰ or 10⁻¹¹ (Flower et al. 1996; Caselli et al. 1997). The lack of a velocity shift between the SiO and the ions for the 5.2 km s⁻¹ component also indicates that we are observing the very early phases of the interaction of the shock precursor. This is supported by the data at the position (0,-20) where the broader SiO profile (see Fig. 1) suggests that in this case a large fraction of the neutrals has already entered the shock.

On the other hand, the detection of [Si II] 34.8 μm emission in L1448-IRS3 (Nisini et al. 2000) shows the existence of a photon-dominated region (PDR) which could be related to the radiative precursor of the J-type shocks (Shull & McKee 1979; Hollenbach & McKee 1989). In fact, the C-type shock models of Chièze et al. (1998) predict a jump discontinuity in the neutral flow in the early stages for time scales ≤10⁴ years. The

UV radiation field of the radiative precursor associated with such J-shock could affect the chemistry of the pre-shocked medium. It might be possible that the ambient SiO emission would be produced by the radiative precursor through the photodesorption of Si from the grains (Schilke et al. 2001). However, the SiO/HCO abundance ratio in the 5.2 km s⁻¹ velocity component is very different from what is observed in PDRs (Schilke et al. 2001).

In summary, the linewidths, velocities, abundances, and spatial distribution of the SiO in L1448-mm/IRS3 could be explained by the radiative and/or magnetic shock precursors associated with the jets driven by protostars. Based on all these results, we speculate that we have probably detected the first evidence of the chemical effects on the ambient cloud produced by the precursors of interstellar shocks. Higher angular resolution observations of SiO, HCO, and tracers of the ambient gas are needed to clearly establish the origin of the ambient emission of SiO in L1448.

This work has been supported by the Spanish MCyT under projects number ESP2002-01627, AYA2002-10113-E and AYA2003-02785-E. We thank J.R. Goicoechea for useful comments and suggestions. We also thank an anonymous referee for helping us to improve the manuscript.

REFERENCES

- Bachiller, R., Cernicharo, J., Martín-Pintado, J., Tafalla, M., & Lazareff, B. 1990, *A&A*, 231, 174
 Caselli, P., Hartquist, T. W., & Havnes, O. 1997, *A&A*, 322, 296
 Chièze, J.-P., Pineau des Forêts, G., & Flower, D. R. 1998, *MNRAS*, 295, 672
 Codella, C., Bachiller, R., & Reipurth, B. 1999, *A&A*, 343, 585
 Curiel, S., Torrelles, J.M., Rodríguez, L. F., Gómez, J. F., & Anglada, G. 1999, *ApJ*, 527, 310
 Draine, B. T. 1980, *ApJ*, 241, 1021
 Flower, D. R., Pineau des Forêts, G., Field, D., & May, P. W. 1996, *MNRAS*, 280, 447
 Hollenbach, D., & McKee, C. F. 1989, *ApJ*, 342, 306
 Irvine, W. M., Goldsmith, P. F., & Hjalmarson, A. 1987, *Interstellar processes*. Hollenbach, D. J., Tromson, H. A. (eds.) Reidel Dordrecht, p. 561
 Lefloch, B., Castets, A., Cernicharo, J., & Loinard, L. 1998, *ApJ*, 504, L109
 Leung, C. M., Herbst, E., & Huebner, W. F. 1984, *ApJS*, 56, 231
 Martín-Pintado, J., Bachiller, R., & Fuente, A. 1992, *A&A*, 254, 315
 Millar, T. J., Herbst, E., & Charnley, S. B. 1991, *ApJ*, 369, 147
 Nisini, B., Benedettini, M., Giannini, T., Codella, C., Lorenzetti, D., Di Giorgio, A. M., & Richer, J. S. 2000, *A&A*, 360, 297
 Pilipp, W., Hartquist, T. W., & Havnes, O. 1990, *MNRAS*, 243, 685
 Pilipp, W., & Hartquist, T. W. 1994, *MNRAS*, 267, 801
 Schenewerk, M. S., Snyder, L. E., Hollis, J. M., Jewell, P. R., & Ziurys, L. M. 1988, *ApJ*, 328, 785
 Schilke, P., Pineau des Forêts, G., Walmsley, C.M., & Martín-Pintado, J. 2001, *A&A*, 372, 291
 Shull, J. M., & McKee, C. F. 1979, *ApJ*, 227, 131
 Ziurys, L. M., Friberg, P., & Irvine, W. M. 1989, *ApJ*, 343, 301